

Only Skin Deep

*Ben S. Cook, T. Le, S. Palacios,
A. Traille, and M.M. Tentzeris*

The ability to monitor and sense environmental conditions in real time over large areas is a difficult and expensive task, especially when it comes to monitoring in harsh environments. Whether it is monitoring suspension bridges that experience immense forces from storms and earthquakes for structural integrity, detecting noxious gases in manufacturing facilities, or making sure the vegetables on the supermarket shelf are still fresh and being kept at the correct temperature and humidity level, these sensors and sensor networks have the ability to greatly improve cognitive intelligence and knowledge of the environment around us, that is, as long as they come at the right price. Current methods for deploying large-scale sensor networks involve miles of cabling that source power and collect data, or battery operated wireless sensors, which pose a serious environmental risk with the disposal of billions of batteries every year. While these methods are necessary in some situations where real-time data or harsh environments prohibit manual monitoring of critical environment parameters, the cost, installation difficulty, and maintenance rarely justify their use over manual inspections and monitoring. This is where the concept

of smart skins comes in. Smart skins are cognitive, intelligent skins that sense, wirelessly communicate, and, in the future, will be able to modify environmental parameters using simple passive RFID technology. These skins can be applied everywhere be it a shelf lining in a grocery store or the outside of a Boeing 787, all while maintaining an unobtrusive and lightweight form factor similar to the application of a decal sticker. Smart skins are zero-power devices meaning they scavenge their own energy using ambient electromagnetic, solar, thermal, mechanical, or RFID/Radar-based interrogation techniques. In short, smart skins could prove to be

Ben S. Cook (Benjamin.cook@gatech.edu), T. Le, S. Palacios, A. Traille, and M.M. Tentzeris (etentze@ece.gatech.edu) are with the School of Electrical and Computer Engineering, Georgia Institute of Technology, Atlanta, Georgia. A. Traille is also with LAAS-CNRS, Toulouse, France.

© PHOTODISC

Digital Object Identifier 10.1109/MMM.2013.2240855
Date of publication: 2 April 2013

The RFID chip can be removed from the sensor integrated antenna entirely and the resonant frequency shift in the backscattered signal can be identified using several methods.

the ultimate sensing tool that could potentially allow for the mass implementation of perpetual wireless networks even in extremely rugged environments. The system overview of a conventional smart skin is shown in Figure 1, which shows a skin consisting of several types of sensors that can be uniquely identified in a sensing matrix, and an interrogation network that is used to poll/interrogate the sensors and relay the data back to a processing hub. This allows real-time knowledge of various sensed parameters, such as the stress gradients due to trucks passing over bridges, or of the propagation rate of a gas leak or fire within a building. The smart skin concept can also be extended to that of body-wearable skins for continuous monitoring and reporting of critical biosignals utilizing novel liquid antenna principles. Biocompatibility and wearability requirements further push the need for autonomous, self-powering sensors.

Building Smart Skins from the Ground Up

Before going into the intricacies of the sensors and wireless sensing mechanisms that enable smart skins, a step back will be taken to the technology that makes producing smart skins possible in a cost-effective way for applications up to tens of gigahertz, which is printing. One of the biggest issues that has inhibited the advancement of smart skins in the past was the inability to fabricate on conformal substrates at scales large enough to cover entire buildings. Typical flex substrate fabrication takes place in a clean-room environment and is a subtractive process meaning patterning and etching are required [1]. Not only is this an expensive process but it has environmental effects due to the hazardous chemicals required. There are inherent size limitations with standard etching processes, which makes large-scale processing almost impossible.

Over the last decade, major advances in printing technology have pushed printing into the mainstream for flexible and conformal electronics fabrication because it eliminates the majority of these issues. Printing is a purely additive process, meaning materials are patterned during deposition eliminating the need for etching and material waste. It is also a manufacturing technology that is scalable via roll-to-roll processing, which is well known for its use in the newsprint industry, an example of which can be seen in Figure 2. Roll-to-roll technology can print conformal skins that are hundreds of meters

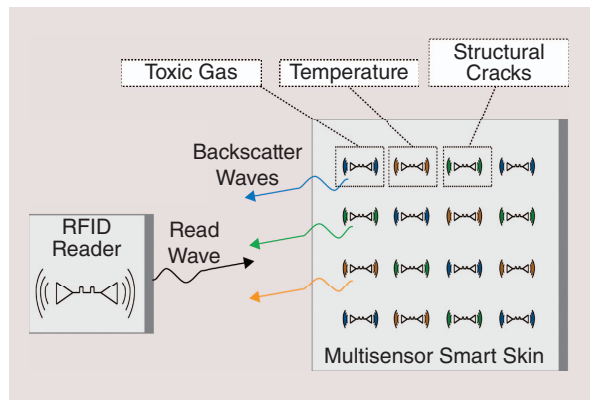


Figure 1. High-level implementation of a smart skin.

long and, in some cases, kilometers if required, making printing an optimal fabrication method. It can also be used with low-cost organic and polymer substrates such as paper, which have the potential to create green smart skins if effective environmentally friendly weather coatings are applied.

Inkjet printing of electronics has been enabled by the discovery of nanoparticle and nano-enabled inks. These nano inks, which consist of nanometer sized particles of metals, carbon nanotubes (CNTs), graphene, or a wide range of semiconducting and polymer compounds, contain particles small enough

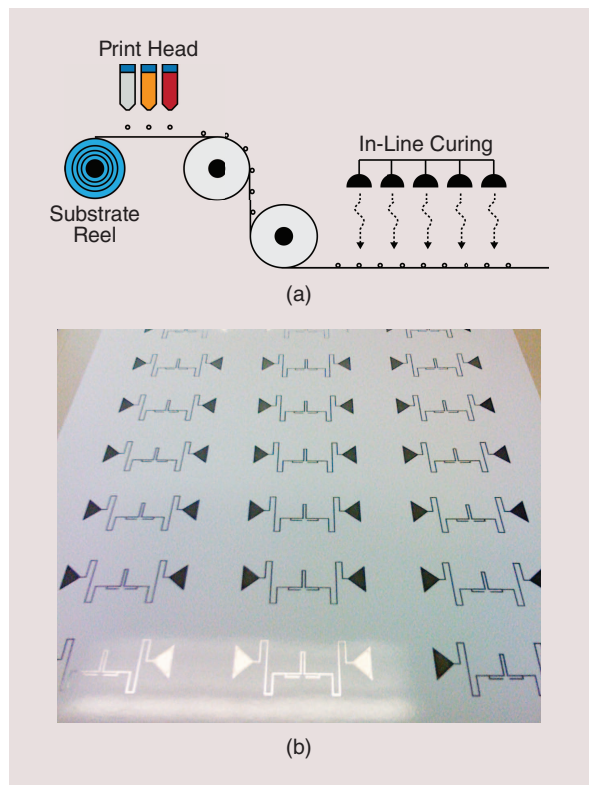


Figure 2. (a) Roll-to-roll inkjet printing process used in an industrial environment and (b) an RFID array printed using an inkjet-printing process, which can be used in smart-skin applications.

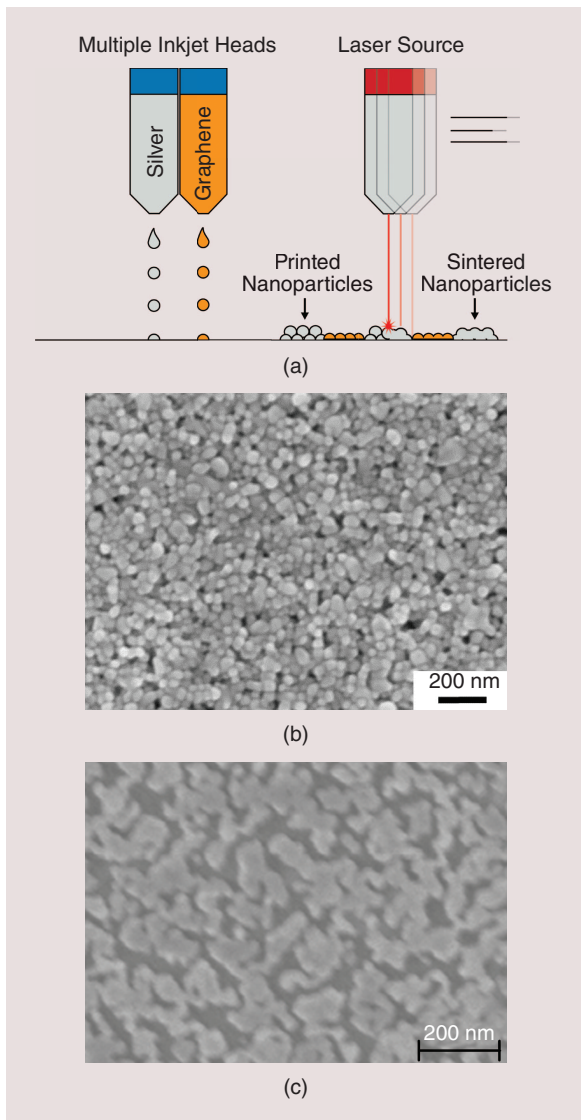


Figure 3. (a) Diagram of an in-line laser sintering process to anneal printed nanoparticles, (b) unsintered printed silver nanoparticles, and (c) sintered nanoparticles.

to be printed through the micron-sized nozzles of an inkjet printer head. Several nozzles can be run at once to pattern multiple materials simultaneously. Once the materials are patterned onto the substrate, curing methods such as heat, laser, or atmospheric modification melt or link the printed nanoparticles into bulk structures [2]–[5]. The entire process can be completed in a matter of minutes allowing for rapid production at large scale. An example of this process is shown in Figure 3.

Because of the wide variety of materials this process can deposit, the use of nano-enabled ink has become very popular for printing RFID integrated antennas, sensors, and even CNT diodes and transistors [3], [6]–[8]. This makes printing a perfect platform for monolithically integrating sensors, antennas, and RFID functionality into smart skins.

CNT composites have been found to be one of the most promising materials for gas sensing due to their large surface-to-volume ratio and surface affinity to bond with gasses such as NH_3 , CO_2 , and NO_x .

RFID Zero-Power Sensing Techniques

When it comes to smart skins and sensing, large, long-term installations come to mind. Wherever these skins are applied, they need to last for a long time and endure moderate to harsh conditions. This means the sensors need to be reliable, energy efficient, and extremely low cost to become a viable long-term solution. They also need to be able to communicate their information wirelessly at a real time or near-real time data rate to be effective. The block diagram of a standard off the shelf wireless sensor is displayed in Figure 4 [9]. The sensor that could be for gas, strain, temperature, or a variety of other variables transforms the physical quantity being measured into an electrical property change. This electrical change could be resistance, reactance, charge carrier density, or a variation in the dielectric constant. The interface circuitry of the sensor reads this electrical change and converts it to a voltage, which an analog to digital converter can read. Once the signal is digitized, it is conditioned and processed in the microcontroller (μC) and then encoded and transmitted via the RF module. The data is then transmitted from the sensors antenna across the wireless transmission path to the reader. It is clear that several of the components in the standard wireless sensing require large amounts of power such as the RF module, the μC , and the amplifiers for the analog interface circuitry. It would be much more beneficial if passive methods such as passive RFID backscatter-based or Radar-based architectures could be utilized to remove power requirements while still incorporating sensing and wireless communication and detection capabilities [10]. Integrating with an RFID architecture has the added benefits of modularity and ease of integration with current RFID off-the-shelf readers, zero-power, Generation 2 Electric Product Code (EPC-GEN2) anti-collision mechanisms, and data-storage capabilities. The following methods covered are solutions to wireless sensor design, which meet the requirements for smart skin integration, which are: unique RFID identification, sensor measurement accuracy and repeatability, and zero-power batteryless architecture.

WISP

The Wireless Identification and Sensing Platform (WISP), which is presented first as an already available off the shelf solution that has been customized for

wireless sensing, is a fully passive, battery-free, and programmable RFID tag [11], [12] that can be powered and read by off-the-shelf EPC-Gen2 UHF RFID readers. It has an on-board microcontroller for sensing and computing functions and is a very function-rich platform. The block diagram of a WISP is shown in Figure 5, showing power harvesting, sensor integration, processing, and modulation/demodulation capabilities. The WISP is solely powered by the RF energy illuminated by any commercial RFID Reader. This RF energy from the reader is rectified with a charge pump topology of diodes and capacitors to charge the on-board capacitor. Whenever located within the interrogation zone of an RFID reader, the WISP-GS is automatically detected and begins transmission of the sensed information within the EPC message of the RFID communication packet. The WISP is a very powerful implementation tool because it is available off-shelf, passive, has processing capabilities, and works with current off the shelf RFID readers making it perfect for smart skin use aside from the fact that it requires several discrete components, which will add to the cost of the skin.

RFID Sensor Integrated Antennas

As with the WISP, most wireless sensor nodes require the interrogation of a wireless module that is separate from the sensor. However, this increases the component count and power budget as additional processing and mixed-signal interfaces are needed. However, if the sensor itself can be used as a wirelessly communicating component, meaning it provides information on the sensed physical quantity by means of a transmitted or back-scattered wireless signal, the additional interface hardware and power consumption can be cut down. There are several methods of doing this, which include introducing a resonant shift (frequency modulation), or amplitude shift (amplitude modulation) in the backscattered signal. The simplest implementation is to iterate or load the antenna that is used by the wireless module for communication with a sensor to modulate the back-scattered signal [6]. This integration drastically cuts cost and system complexity by removing the majority of the required components and leaving only the sensor-integrated antenna and the RFID communication chip.

The sensor, which can be modeled as a complex impedance is used to load the arms of a dipole. A change in the impedance of the sensor by chemical, mechanical, or electrical stimuli causes the antennas resonant frequency to change.

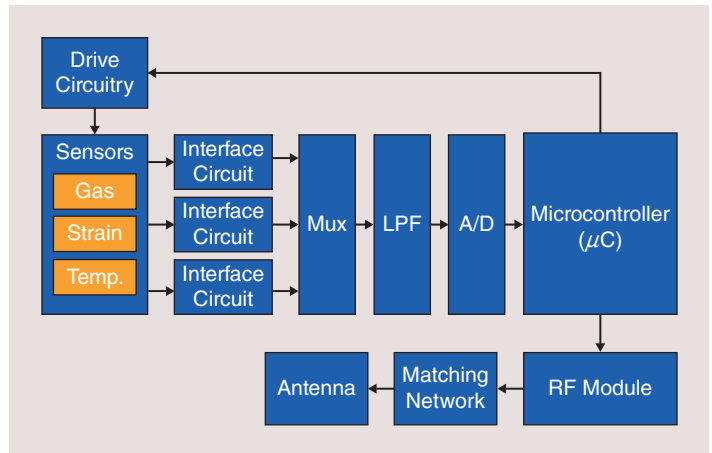


Figure 4. Block diagram of the typical wireless sensor node.

If the impedance change of the sensed physical parameter on the sensor is characterized, the frequency shift of the backscattered signal can be converted back into a physical shift from the sensed quantity.

Chipless RFID Antenna Backscatter

Going even one step further in simplicity, the RFID chip can be removed from the sensor integrated antenna entirely and the resonant frequency shift in the backscattered signal can be identified using several methods including multiresonator chipless RFID [13], time gated delayed resonance [14], [15], backscattered power [6], and diode frequency doubling [16], [17]. While these methods are by far the simplest and lowest cost methods available, they are more vulnerable to multipath and environmental effects as digital modulation schemes are not employed on the sensor end. However, if these methods are used in an uncluttered environment such as on the external walls of a large building multipath effects are much less prevalent.

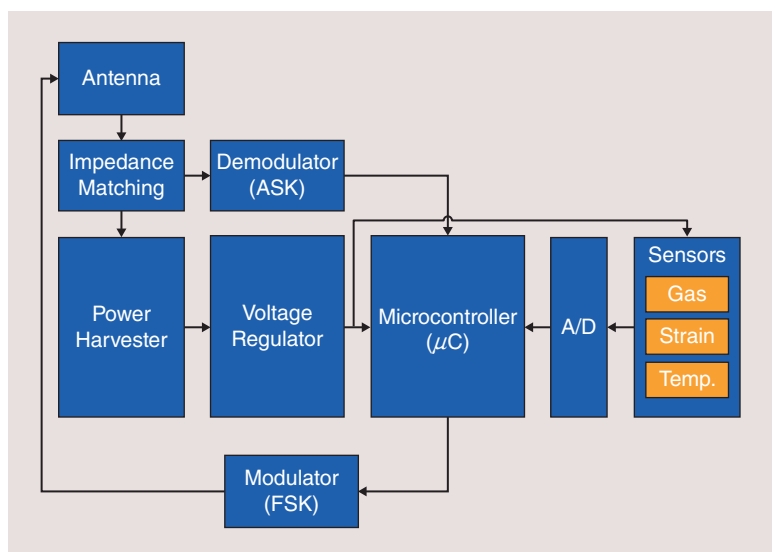


Figure 5. Block diagram of the WISP RFID wireless sensor platform.

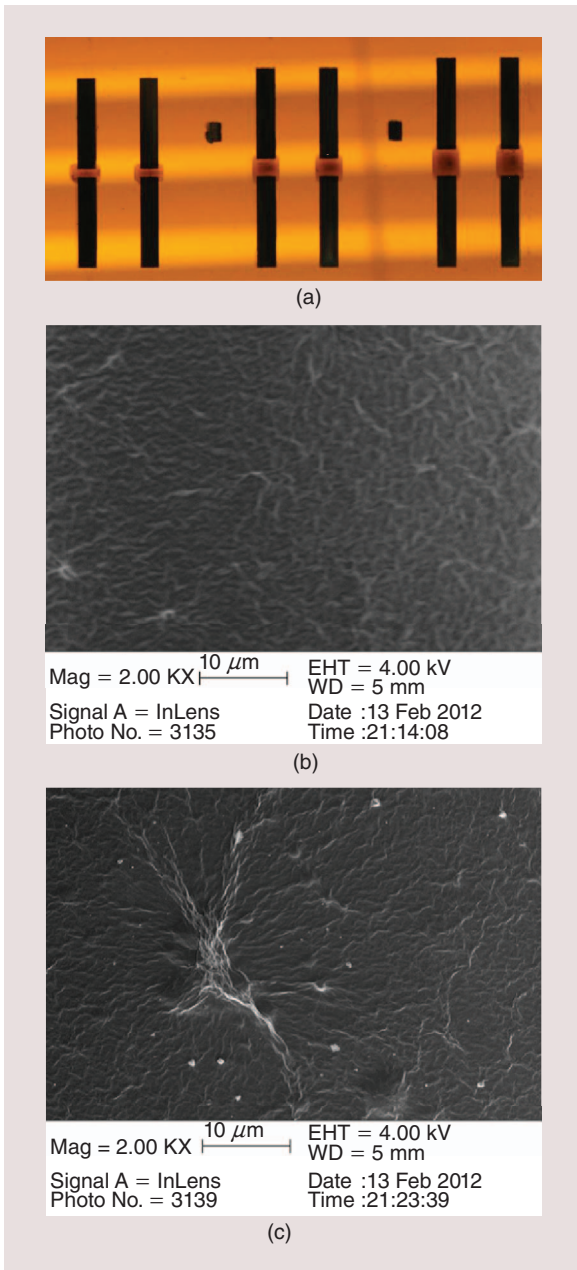


Figure 6. (a) Three different dimension graphene patterns interfaced with silver nanoparticle conductive lines, (b) printed GO before reduction, and (c) reduced GO [11].

Implementing Nanotechnology-Enabled Gas Sensing for Smart Skins

All of these sensing mechanisms are, in the end, needed to interface with sensors to extract data on specific sensed quantities and report back to the end user. One of the critical sensing applications for smart skins is the detection of gasses such as ammonia (NH_3), nitrogen dioxide (NO_2), and carbon monoxide (CO). NH_3 is a major concern in areas of high agricultural activity as it is a natural byproduct of livestock and is also produced by a number of industrial sources linked with agriculture. It is also a key

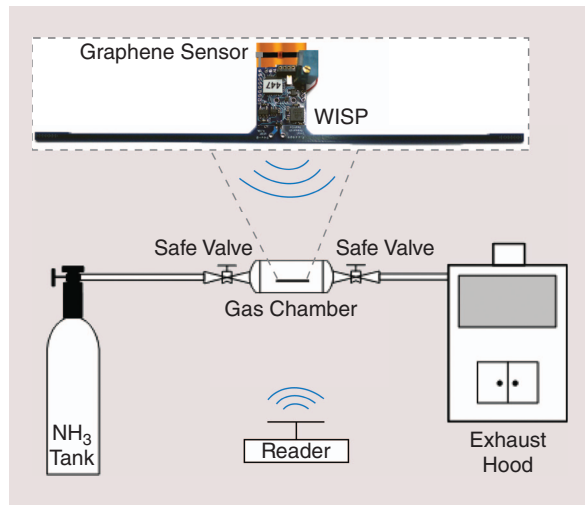


Figure 7. System-level diagram of the gas measurement setup including a WISP graphene gas sensor, reader, and gas containment chamber.

indicator of spoiling foods, which has applications in supermarkets and food transport. Other gasses, such as NO_2 and CO , are hazardous to humans and wildlife and are contributors to acid rain and smog formation [9]. Recently, advances in nanotechnology have created the ability to print gas sensors using CNTs and graphene/graphene oxide (GO) sheets. CNTs and graphene sheets have been the recent focus of researchers for ultra-sensitive gas detection [11]. CNT composites have been found to be one of the most promising materials for gas sensing due to their large surface-to-volume ratio and surface affinity to bond with gasses such as NH_3 , CO_2 , and NO_x . The combination of high surface to volume ratio and easy adsorption of these gasses causes significant changes in the electrical impedance of the CNTs upon exposure. Selective functionalization can also be performed to allow CNTs to detect gasses individually.

Graphene is a single layer of carbon atoms oriented in a planar fashion. It has high mobility ($200,000 \text{ cm}^2/\text{V-s}$), is extremely strong, and also boasts a high thermal conductivity. What makes it such a good gas sensor is that it is a zero band gap semiconductor, which means small variation in charge carrier densities lead to noticeable changes in conductivity. It is so sensitive that single gas molecule detection has been demonstrated [11]. It is also an inherently low-noise material giving it added benefits as a sensor.

As both graphene and CNTs change their electrical properties upon contact with certain gasses, they are ideal for integration with several of the aforementioned RFID based sensing methods. Various detection methods based on zero-power RFID and chipless methods have been employed using CNT and graphene sensors, which can be integrated with smart skins for remote and real-time gas sensing.

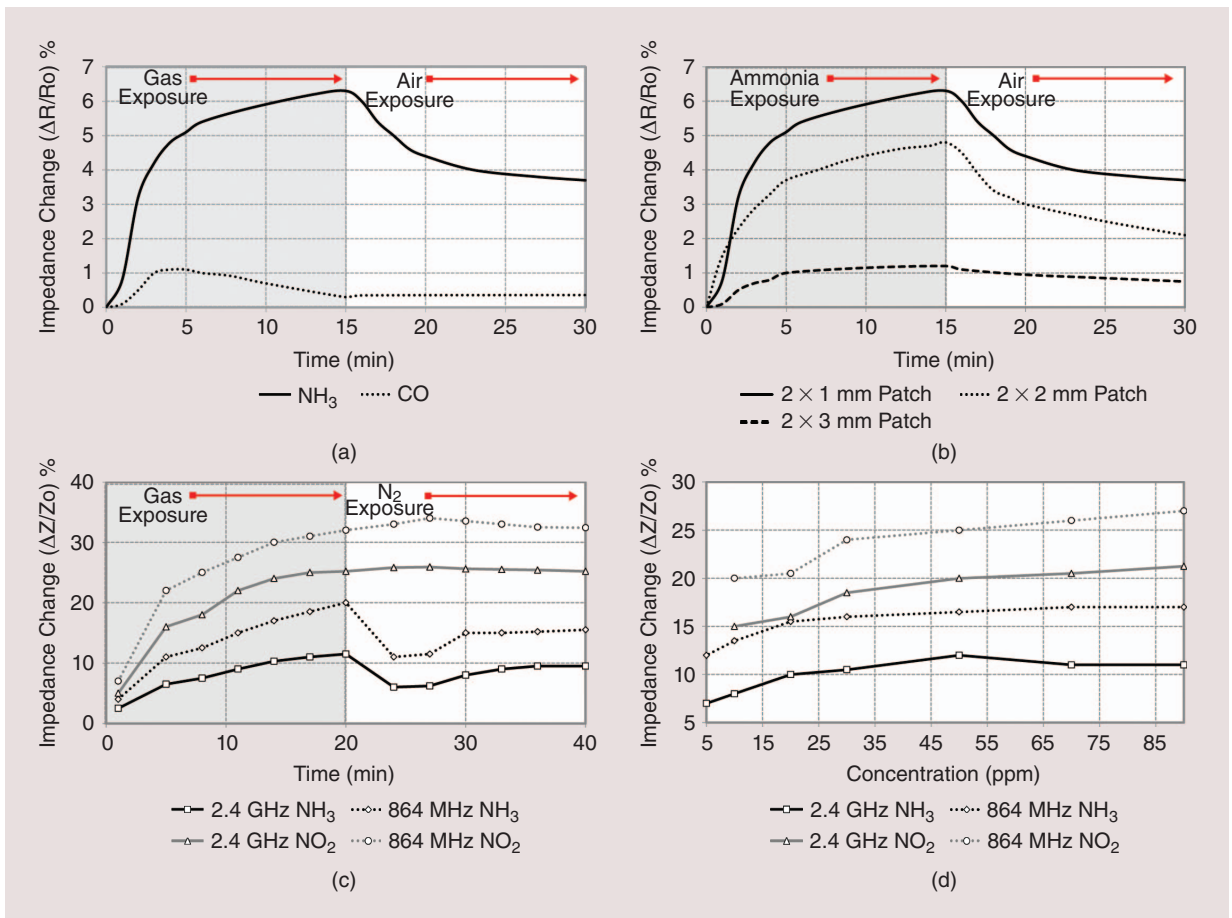


Figure 8. (a) Graphene sensitivity to different gas exposure, (b) graphene sensitivity over time with different dimension patterns, (c) MWCNT response to gas over time, and (d) MWCNT response to different parts per million (ppm) levels.

Graphene-Based WISP Gas Sensor

Graphene has many properties favorable to gas sensing, however, deposition is usually costly. Recent developments in producing graphene based inks by Le et al. [11] have enabled the implementation of an inkjet-printed graphene gas detection sensor that has a very rapid recovery time and high sensitivity. As demonstrated in [11], GO, which is the precursor to graphene is inkjet-printed onto a UV-ozone treated Kapton substrate with silver contact pads. The printed GO is then inserted in post processing to reduce the GO to sheets of reduced graphene oxide (RGO). Sintering using heat and laser can both be used for this process [18]. The deposited graphene sensors can be seen Figure 6 with silver nanoparticle pads, which are used to connect the sensor with the WISP RFID tag.

As the conductivity of the reduced graphene changes upon exposure to gas, the graphene sensor is used in a resistor divider configuration with a fixed resistor, which is placed across the WISPs regulated 1.8 V and ground rails. When the WISP is interrogated by the reader, the voltage from the voltage divider circuit is read by the WISPs analog to digital converter

(ADC), processed, and sent to the reader in the EPC-Gen2 packet.

The WISP gas sensor is placed in an isolated gas chamber, as shown in Figure 7, to expose the sensor to extremely small amounts of NH_3 and CO to determine the sensitivity. Figure 8(a) and (b) show the extracted sensitivity, which is the change in dc impedance of the sensor over the initial impedance. Changes of up to 6% are realized with response times of less than five minutes when NH_3 is applied. Upon removal of the gas at $t = 15$ minutes and application of air, the sensors recover 30% within five minutes. This allows for re-use of the sensors, which is required for low-cost long-term end solutions. Figure 8(a) shows the selectivity of the film between CO and NH_3 showing a noticeable difference in the characteristic response of the sensor to each gas. This can be used in data analysis to back out the type of gas present and exposure amount. Similarly, multiwalled CNTs (MWCNT) can be used as the sensor load for the WISP as is demonstrated in [19]. This sensor uses MWCNTs printed on a paper substrate to induce the impedance change upon exposure to gas. The inkjet-printed MWCNT

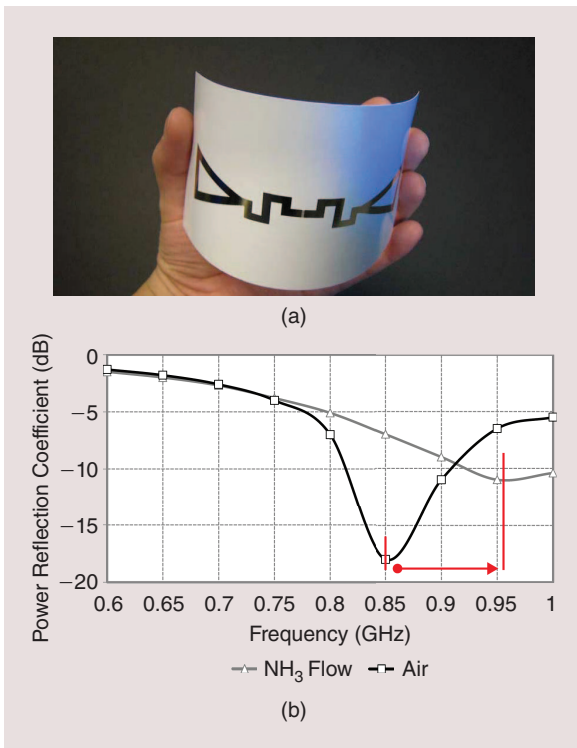


Figure 9. (a) Inkjet-printed RFID tag with SWCNT load in the middle and (b) backscattered power versus frequency for the RFID tag in ambient and under gas exposure.

sensors shown in Figure 8(c) and (d) display relative impedance changes of up to 30% upon exposure to NH₃ and NO₂, which allows for very easy detection and selectivity of gasses.

CNT Loaded RFID Tag Sensors

While the WISP is demonstrated to be a feature rich RFID solution for extracting sensor data using a zero-power approach, and is very useful for small-scale applications, large-scale smart skins require that the sensor designs are cheaper and easier to fabricate. A sensor utilizing single-wall CNTs (SWCNTs) to load an RFID tag has been demonstrated by Yang et al. in [6], which reduces cost and fabrication complexity significantly.

The sensor that is shown in Figure 9(a) consists of an inkjet printed RFID tag and a printed SWCNT sensor used as a load impedance for the printed RFID antenna. The simplicity of this solution lies in the fact that the antenna and SWCNT sensor can be printed simultaneously in the processing line. The sensor works on the principle of backscattered power to determine resonant frequency shifts caused by the SWCNT load. Backscattered power sensing consists of interrogating the tag with an RF signal over a specified frequency band. The IC chip used in standard RFID tags changes the impedance at the load of the antenna to modulate the backscattered power coefficient (η), which is defined in (1):

Many long-standing structures such as bridges are subject to cyclic loading and thermal stresses caused by the change in seasons, which lead to deterioration and stress fractures.

$$\eta = \left| \frac{Z_{\text{load}} - Z_{\text{antenna}}^*}{Z_{\text{load}} + Z_{\text{antenna}}} \right|^2 \quad (1)$$

where (η) represents the reflection coefficient, and (Z_{antenna}) represents the impedance of the antenna terminals, with (*) being its complex conjugate. The reflected power from the tag at a specified frequency is then product of the incident power on the tag and the power reflection coefficient (η)

$$P_{\text{Backscatter}} = \eta P_{\text{Incident}} \quad (2)$$

So as the frequency dependent load impedance changes, the backscattered power over the frequency band also changes.

When the IC is replaced with the SWCNTs, the SWCNT load acts as a variable impedance when exposed to varying levels of gas as shown previously. By changing the loading impedance, the resonant frequency and thus backscattered power are changed, and by measuring the backscattered power over a specified frequency band, the change resonant frequency of the sensor can be determined.

The printed RFID tag with SWCNT load shown in Figure 9(a) is a meander bow tie dipole designed for the 868 MHz RFID band that has an input impedance matched to that of the 50 ω printed sensor. SWCNTs are printed in the center gap of the tag to use as the variable load. The tag is placed in a controlled gas chamber and exposed to NH₃ gas. A dielectric probe fixture is used to measure the power reflection coefficient of the tag before and after exposure. As shown in Figure 9(b), the tag experiences a 100 MHz shift in resonant frequency after exposure to the gas. This sensitivity is large enough to make real-world implementation of these chipless tags feasible.

Implementing Strain Sensing for Smart Skins

A second important sensing quantity targeted by smart skins is structural strain and cracking as there are extremely high costs and liabilities associated with the failure of dams, bridges, aircraft, and skyscrapers. Many long-standing structures such as bridges are subject to cyclic loading and thermal stresses caused by the change in seasons, which lead to deterioration and stress fractures. According to [20] 50–90% of all large-scale structural failures are due to fatigue cracking. Constant inspection

While current technologies have enabled low-cost smart skins which were nearly impossible to produce ten years ago, work is currently underway to make smart skins even cheaper and eventually wearable.

of these large structures is required to keep them operational and ensure they are safe for use. Failures or down time due to required inspections can present significant costs in time and resources and periodic manual inspections by personnel, which are primarily visual, are difficult and unreliable in some situations where there are hard to access areas or cracks underneath paint. Several sensing techniques that are in use such as ultrasonic interrogation, eddy-current sensors, and comparative vacuum sensors [21] are expensive to implement on a large scale due to labor and wiring costs. A WISP based strain sensor using foil strain gauges has also been implemented, but the complexity of installing thousands of WISPs over a large structure is costly. Recently several methods using patch antennas have been used to detect strains down to microstrain using patch antennas. These methods have also been demonstrated to detect structural cracking along with crack orientation and magnitude [14], [15], [21], [22].

RFID Integrated Patch Antenna Strain Sensor

Simpler and lower cost than implementing a fully functional WISP strain sensor, the sensing mechanism is integrated into the antenna as with the aforementioned gas-sensing RFID antenna. However, this antenna integrated sensor works on the principle of electrical length change in patch antennas caused by an applied strain instead of load impedance change as demonstrated in [23]. Strain is defined as the change in length over the initial length of an object and occurs when a tension or compression is exerted

$$\epsilon = \frac{\Delta L}{L}. \quad (3)$$

As patch antennas have a resonant frequency that is dependent on the physical length of the patch and the dielectric constant of the substrate (4), a strain, which changes the length of the patch should also produce a shift in the resonant frequency of the antenna. By mounting an RFID tag on the patch antenna, an RFID reader can be used to read the backscattered power over a frequency range and determine the strain that is being experienced by the sensor by the shift in resonant frequency

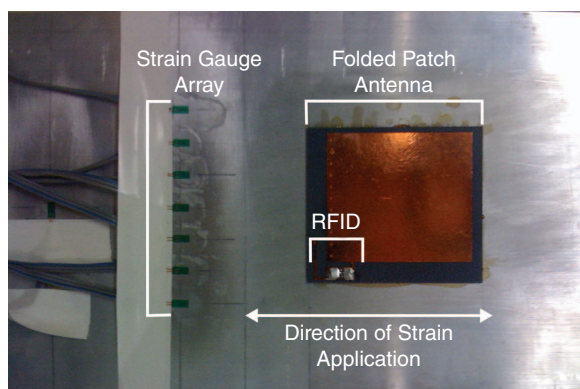


Figure 10. Printed RFID folded patch antenna used for strain sensing mounted on an aluminum plate for applying strain.

$$f_0 = \frac{c}{4(L + L')\sqrt{\epsilon_r}}. \quad (4)$$

The patch antenna used for the sensor is displayed in Figure 10. It is a folded patch, which is used to miniaturize the overall size and match the impedance of the antenna to that of the RFID chip. The antenna is printed on a Kapton substrate as it is thin and allows for a good strain transfer to the patch when it is mounted on the stressed structure.

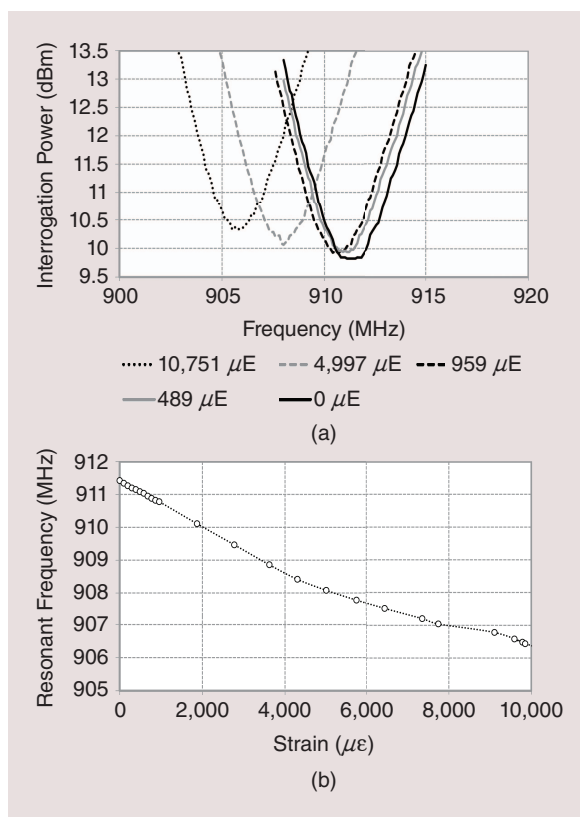


Figure 11. (a) Interrogation power versus frequency of the RFID folded patch under varying levels of strain and (b) the extracted resonant frequency of the patch versus strain.

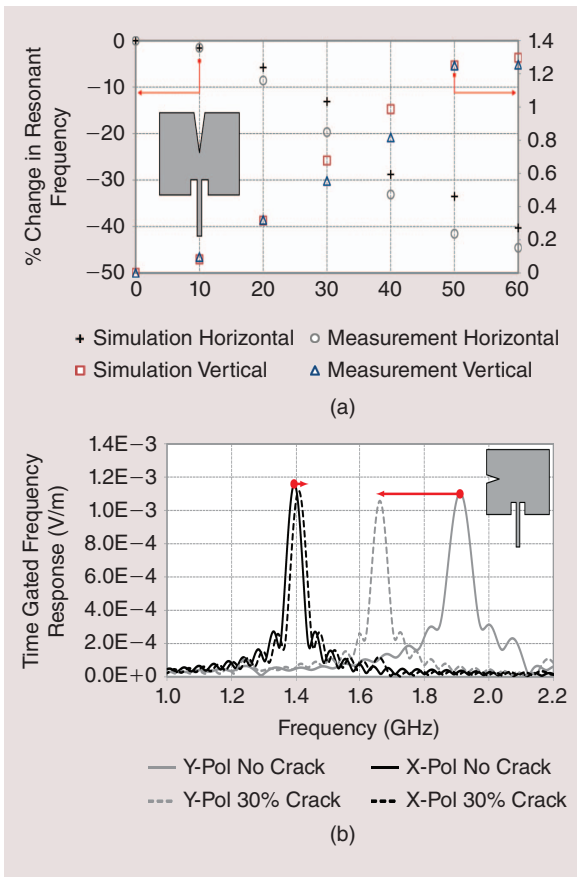


Figure 12. (a) Resonant frequency shifts in the vertical current mode of a patch when a crack forms horizontally and (b) the results of wirelessly interrogating both the horizontal and vertical modes of the patch using the time-gating method.

To test the antenna, the antenna is mounted on an aluminum specimen to which defined values of stress and therefore strain are applied. Foil strain gauges are also placed on the aluminum specimen for a baseline calibration measurement of the applied strain. The measurement setup consists of a Voyantic Tagformance RFID reader placed 30 cm away from the RFID patch antenna mounted on the aluminum specimen. Discrete strain levels are applied

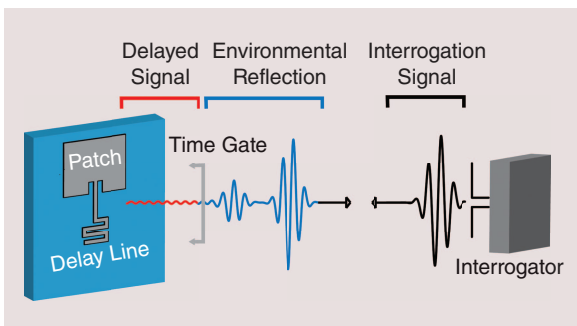


Figure 13. Chipless method of measuring the resonant frequency of a patch for crack detection in structures.

to the specimen with a tensile testing machine and the RFID reader performs a frequency sweep of the backscattered power from the RFID tag at each strain level. The measured backscattered power, which is displayed in Figure 11(a) shows the decrease in resonant frequency of the RFID patch antenna as the strain level increases. This correlates with (4) as the patch is lengthening under strain, which makes the antenna electrically longer.

The resonant frequency of the patch is fitted against the applied strain level in Figure 11(b). There is a general linearly decreasing trend in the resonant frequency with applied strain, which is to be expected. The sensor has a gauge factor of 0.77, which is the change in resonant frequency over the change in strain with a linearity of above 0.9. Typical powered strain gauges have a gauge factor of 1.2, so this passive sensor provides similar sensitivities to that of fully powered strain sensing solutions.

Chipless Antenna Integrated Crack Sensor

Along with measuring strain, structural cracks are an important quantity to measure as cracks are an immediate danger on large structures. Again, in this sensor a patch antenna is used to detect cracks, in a chipless, backscatter technique using time-domain measurements. Patch antennas exhibit the unique quality of having horizontal and vertical modes, the resonance of which can be set by the length and width dimensions of the structure. If a single polarization antenna is used to excite the patch, the two different modes can be interrogated independently by orienting the polarization of the interrogation antenna with the desired mode of the patch. This is useful as when cracks form through a patch, they will form vertically, horizontally, or on an angle to the two axis of the patch antenna.

As the resonant frequency of each mode (horizontal and vertical currents) is dependent on the electrical length of the patch, a crack will cause mode perturbations, which are different in the currents of the horizontal and vertical-current modes of the patch. For example, a crack in the horizontal direction will have little impact on the flow of currents in the horizontal direction, however, currents in the vertical direction will have to flow around the crack, which increases the electrical path length of the vertical mode. This means interrogation of the horizontal mode will show little change in the resonant frequency while the vertical mode will show a decrease due to the increase in path length for the current.

In [14], patch antennas are inkjet printed on paper substrate and cracks are introduced with a variety of shapes and orientations in the patch. Figure 12(a) shows the resonant shifts in an inkjet-printed patch, which has a vertical resonance of 1.9 GHz and a

One promising area of research into novel antenna designs that will enable efficient WBANs is targeting liquid-based antennas.

horizontal resonance of 1.4 GHz. It can be seen that when the horizontal crack, which is perpendicular to the vertical mode forms, it causes drastic shifts downward in resonant frequency of up to 50% as the current has to travel around the crack to reach the top of the patch. This makes detecting cracks very simple as the shifts in resonance are large. Cracks that form in the vertical direction have very little effect on the resonant frequency of the vertical patch mode causing only 2–3% shifts upward in frequency as the currents are displaced very little.

To measure these resonant frequency shifts, a chipless method is used to reduce cost, which employs time gating of a backscattered wideband Gaussian pulse. A reader sends a Gaussian pulse, which contains all of the frequencies in a band of interest. The pulse hits the patch, which has a delay line attached. An initial reflection of the pulse off of the patch and surrounding environment such as the bridge the patch is mounted on returns back towards the reader. But, because of the delay line and the highly resonant nature of the patch, a delayed resonance continues from the patch after the initial backscatter, which can be captured by the reader.

Once the time domain reflection is captured, the reader gates out the initial environmental backscatter, and performs a fast Fourier transform (FFT) on the time-gated data. This data gives the resonant frequency of the patch in whichever mode the reader antenna excites. Figure 13 shows the time domain pulse received back at the reader and the region where the data is gated. Figure 12(b) shows the FFT of time-gated pulses in the horizontal and vertical directions with and without the presence of a crack.

As the crack forms in the horizontal direction, the vertical mode has a shift downwards in resonant frequency, while the horizontal mode has a slight upwards shift. These results show successful readings that can detect cracks in a multitude of directions as well as extrapolate the magnitude of the crack.

Future Directions

While current technologies have enabled low-cost smart skins, which were nearly impossible to produce ten years ago, work is currently underway to make smart skins even cheaper and eventually wearable. Two areas of development currently underway include integrating WISP-like sensor modules onto inkjet-printed paper skins, which will make feature rich platforms available at a much lower cost, and enhancing wearable on-body antenna efficiencies through the use of liquid antennas in order to enable wearable wireless body area networks (WBAN) and real-time medical monitoring systems.

Smart Wireless Integrated Module

As demonstrated previously, feature-rich RFID platforms such as the WISP make wireless sensing a trivial

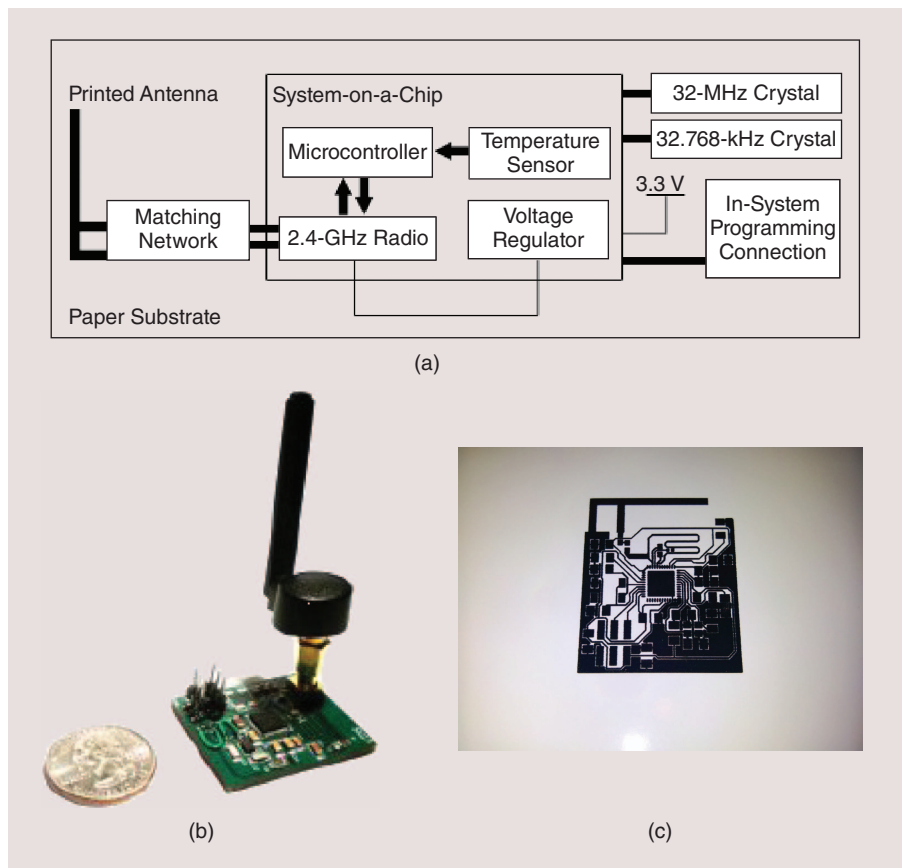


Figure 14. (a) System level diagram of the smart wireless integrated module (SWIM), (b) off-the-shelf version of the SWIM with external antenna, and large form factor, and (c) paper printed SWIM, which has planar inverted-F antenna (PIFA) integrated antenna to miniaturize overall form factor.

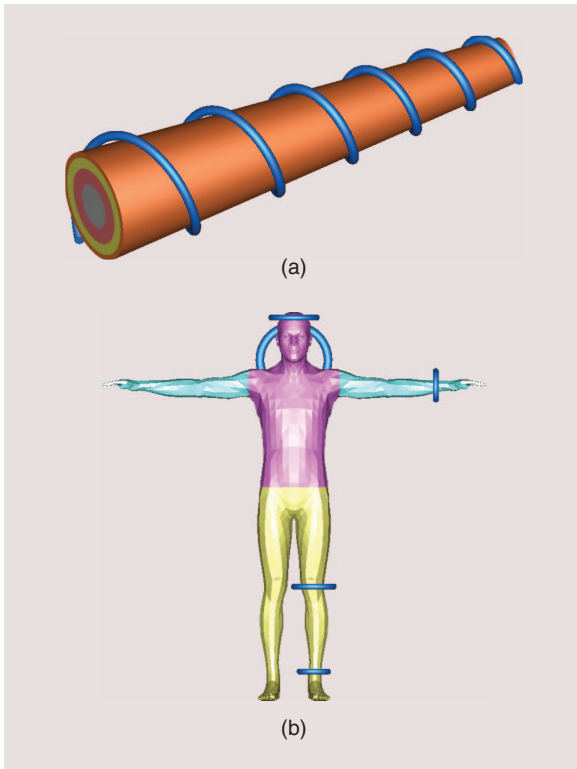


Figure 15. (a) Liquid antenna wrapped around a forearm body phantom and (b) body model with several ionic liquid antennas.

task, but at the expense of having printed circuit boards and most likely more features than needed. This leads to a price point, which is not cost efficient for large-scale sensing. However, if the entire module is integrated onto a paper or organic polymer substrate and stripped of the extra features, the cost skyrockets down and the sensors become flexible and easy to produce. The SWIM, which is shown in Figure 14 is an initial prototype of a WISP-like sensor, which has been ported to inkjet-printed substrates [24].

It is a stripped down version of the module in Figure 14(b) employing the system-on-chip (SOC) concept and has an RF module, μC , analog to digital converters, and on-board integrated antenna. With advances in printed passives and transistors [7], [25], these systems will one day be able to be fully printed down to the transistor level as has been demonstrated by recent prototypes [26].

Liquid Antennas for Wearable Skins

On the forefront of smart skins is the body-wearable skin that performs real-time medical sensing and reporting [27], which is an extension of the WBAN. However, one of the major issues with wearable skins is that on-body wireless communication suffers from the appreciable RF losses due to the high permittivity and loss of body tissues [28]. It is well known that large mismatches in permittivity cause surface

Cognitive printed smart skins have the potential to greatly increase the safety and longevity of large structures, increase quality of life in everyday environments such as grocery store food aisles, and provide a wealth of knowledge all in a low-cost, unobtrusive manner.

waves, which degrade radiation and increase substrate based losses. One promising area of research into novel antenna designs that will enable efficient WBANs is targeting liquid-based antennas. Like printing, liquid-based antenna manufacturing is another simple, additive, environmentally friendly and nontoxic process. The liquid antenna consists of a flexible biocompatible container or tube filled with a dielectric liquid (e.g. saline). The liquid-based structure will provide the necessary flexibility for integration into conformal smart-skins, with the additional features; reconfigurability and enhanced performance within the vicinity of high permittivity tissues. The reconfigurability comes from being able to fill, drain, and reconfigure the water filled structure. Enhanced performance is due to their inherent high permittivity, which allows for more-efficient radiation and better RF matching with the surrounding tissues. The liquid antenna itself can also function as a sensor because it can interact with the body to change their radiation properties such as with changes in temperature, blood pressure, and sweat contents if selectively permeable membranes are used. Liquid-filled plastic or glass antennas work on the principle of dielectric cavity resonance where a cavity of fluid is excited at its resonant frequency to produce a radiating structure. An example of a biologically inspired liquid based antenna shown in Figure 15 is a spiral wrapped around an arm phantom, which is filled with a salt water solution. By adjusting the salinity levels, the permittivity and conductivity of the cavity can be controlled for optimal matching with the body. Studies on the radiation performance found that compared with a metal antenna of the same dimensions, which exhibits a radiation efficiency of 26%, the liquid antenna exhibits a 59% radiation efficiency at 1.7 GHz. The improvement in performance and mechanical benefits of the liquid antenna make it ideal for wearable smart skins. The liquid antenna can be mounted on, sewn through, or submerged within a membrane or fabric so that it can be filled and drained while staying intact. Liquid antennas and liquid electronics are an essential and promising component for wearable smart skins.

They will bring to practice new flexible, small-scale, bio inspired, wearable designs that would otherwise be extremely difficult to fabricate.

Summary

Several sensing topologies have been presented for gas and strain sensing for integration with large-scale smart skins. These sensors all exhibit the important properties of zero-power operation, high sensitivity, and some can even be fully implemented in-line with an industrial printing process to enable the manufacturing of low-cost and large form factor skins. Cognitive printed smart skins have the potential to greatly increase the safety and longevity of large structures, increase quality of life in everyday environments such as grocery store food aisles, and provide a wealth of knowledge all in a low-cost, unobtrusive manner. In addition, by using an industry standard RFID platform for sensing, we can leverage the low-cost, low-power benefits of the platform along with the ease of integration with current and future RFID installations. Advances in printed system integration and on body liquid-antenna based wireless sensing will eventually lead to wearable skins that can monitor, sense, and interact with the world around us in a perpetual way, thus significantly enhancing ambient intelligence and quality of life.

References

- [1] G. Wiederrecht, *Handbook of Nanofabrication*. New York: Elsevier, 2009.
- [2] B. S. Cook and A. Shamim, "Inkjet printing of novel wideband and high gain antennas on low-cost paper substrate," *IEEE Trans. Antennas Propag.*, vol. 60, no. 9, pp. 4148–4156, 2012.
- [3] L. Yang, A. Rida, R. Vyas, and M. M. Tentzeris, "RFID tag and RF structures on a paper substrate using inkjet-printing technology," *IEEE Trans. Microwave Theory Tech.*, vol. 55, no. 12, pp. 2894–2901, 2007.
- [4] M. L. Allen, M. Aronniemi, T. Mattila, A. Alastalo, K. Ojanpera, M. Suhonen, and H. Seppa, "Electrical sintering of nanoparticle structures," *Nanotechnology*, vol. 19, no. 17, pp. 1–4, 2008.
- [5] P. Laakso, S. Ruotsalainen, E. Halonen, M. Mntysalo, and A. Kempainen, "Sintering of printed nanoparticle structures using laser treatment," VTT Tech. Res. Centre Finland, Espoo, Finland, Tech. Rep., 2009.
- [6] L. Yang, A. Rida, and M. M. Tentzeris, "Design and development of radio frequency identification and RFID-Enabled sensors on flexible low cost substrates," *Synth. Lect. RF/Microwaves*, vol. 1, no. 1, pp. 1–89, 2009.
- [7] J. Vaillancourt, "All ink-jet-printed carbon nanotube thin-film transistor on a polyimide substrate with an ultrahigh operating frequency of over 5 GHz," *App. Phys. Lett.*, vol. 93, no. 24, p. 243301, 2008.
- [8] R. Vyas, V. Lakafosis, H. Lee, G. Shaker, L. Yang, G. Orecchini, A. Traille, M. Tentzeris, and L. Roselli, "Inkjet printed, self powered, wireless sensors for environmental, gas, and authentication-based sensing," *IEEE Sens. J.*, vol. 11, no. 12, pp. 3139–3152, 2011.
- [9] T. Thai, L. Yang, and M. M. Tentzeris, "Nanotechnology enables wireless gas sensing," *IEEE Microwave Mag.*, vol. 12, no. 4, pp. 84–95, 2011.

- [10] H. Aubert, F. Chebila, M. Jatlaoui, T. Thai, H. Hallil, A. Traille, S. Bouaziz, A. Rifai, P. Pons, P. Menini, and M. M. Tentzeris, "Wireless sensing and identification of passive electromagnetic sensors based on millimetre-wave FMCW radar," in *Proc. IEEE RFID-TA Conf.*, 2012, pp. 398–403.
- [11] T. Le, V. Lakafosis, Z. Lin, C. P. Wong, and M. M. Tentzeris, "Inkjet-printed graphene-based wireless gas sensor modules," in *Proc. IEEE 62nd ECTC Conf.*, 2012, pp. 1003–1008.
- [12] F. Gascoa, P. Ferabolia, J. Braunb, J. Smith, P. Sticklerd, and L. DeOtoe, "Wireless strain measurement for structural testing and health monitoring of carbon fiber composites," *Composites A Appl. Sci. Manuf.*, vol. 42, no. 9, pp. 1263–1274, 2011.
- [13] S. Preradovic and N. Karmakar, "Multiresonator based chipless RFID tag and dedicated RFID reader," in *Microwave Symp. Digest, IEEE MTT-S Int.*, 2010, pp. 1520–1523.
- [14] B. S. Cook, A. Shamim, and M. M. Tentzeris, "A passive low-cost inkjet-printed smart skin sensor for structural health monitoring," *IET Microwaves, Antennas Propagat.*, vol. 6, no. 14, pp. 1536–1541, 2012.
- [15] U. Tata, H. Huang, R. L. Carter, and J. C. Chiao, "Exploiting a patch antenna for strain measurements," *Meas. Sci. Technol.*, vol. 20, no. 1, pp. 1–7, 2009.
- [16] S. M. Presas, "Microwave frequency doubler integrated with miniaturized planar antennas," Ph.D. dissertation, Dept. Elect. Eng., Univ. South Florida, Tampa, FL, 2008.
- [17] X. Yi, B. S. Cook, C. Cho, J. Cooper, Y. Wang, and M. M. Tentzeris, "Passive frequency doubling antenna sensor for wireless strain sensing applications," in *Proc. ASME Conf. Smart Materials, Adaptive Structures Intelligent Systems SMASIS*, 2012, pp. 1–3.
- [18] L. Le, "Graphene supercapacitor electrodes fabricated by inkjet printing and thermal reduction of graphene oxide," *Electrochem. Commun.*, vol. 13, no. 4, pp. 355–358, 2011.
- [19] V. Lakafosis, "Wireless sensing with smart skins," *IEEE Sens.*, pp. 623–626, Oct. 2011.
- [20] C.-H. Foong, M. Wiercigroch and W. F. Deans, "Novel dynamic fatigue testing device: Design and measurements," *Meas. Sci. Technol.*, vol. 17, no. 8, p. 221826, 2006.
- [21] I. Mohammad and H. Huang, "Monitoring fatigue crack growth and opening using antenna sensors," *Smart Mater. Struct.*, vol. 19, no. 5, p. 055023, 2010.
- [22] I. Mohammad, V. Gowda, H. Zhai, and H. Huang, "Detecting crack orientation using patch antenna sensors," *Meas. Sci. Technol.*, vol. 23, no. 1, p. 015102, 2012.
- [23] X. Yi, J. Cooper, V. Lakafosis, R. Vyas, Y. Wang, R. Leon, and M. Tentzeris, "Wireless strain and crack sensing using a folded patch antenna," in *Proc. 6th European Conf. Antennas Propagation*, 2012, pp. 1678–1681.
- [24] S. Palacios, A. Rida, S. Kim, S. Nikolaou, S. Elia, and M. M. Tentzeris, "Towards a smart wireless integrated module on flexible organic substrates using inkjet printing technology for wireless sensor networks," in *Proc. IEEE Int. Workshop Antenna Technology*, 2012, pp. 20–23.
- [25] J. Limb, J. Kima, Y. J. Yoonb, H. Kimb, H. G. Yoonc, S.-N. Leed, and J. Kimb, "All-inkjet-printed metal-insulator-metal capacitor," *Current Appl. Phys.*, vol. 12, no. 1, pp. e14–e17, 2012.
- [26] M. Jung, J. Kim, J. Noh, N. Lim, C. Lim, G. Lee, J. Kim, H. Kang, K. Jung, A. Leonard, J. Tour, and G. Cho, "All-printed and roll-to-roll-printable 13.56 MHz operated 1-bit tag on plastic foils," *IEEE Trans. Electron. Devices*, vol. 57, no. 3, pp. 571–580, 2010.
- [27] D.-H. Kim, N. Lu, Y.-S. Kim, and R.-H. Kim, "Epidermal electronics," *Science*, vol. 333, no. 6044, pp. 838–843, 2011.
- [28] E. Reusens, W. Joseph, B. Latre, B. Braem, G. Vermeeren, E. Tanghe, and L. Martens, "Characterization of on-body communication channel and energy efficient topology design for wireless body area networks," *IEEE Trans. Inform. Technol. Biomed.*, vol. 13, no. 6, pp. 933–945, 2009.

